Proceedings of the 22nd National and 11th International ISHMT-ASME Heat and Mass Transfer Conference December 28-31, 2013, IIT Kharagpur, India

HMTC1300551

MOBILITY OF AIR BUBBLE ENTRAPPED THROUGH JET IMPINGEMENT

Ajay Kawade
M-Tech Student, NIT Rourkela
Rourkela, Odisha, 769008
ajay.kawade7@gmail.com

Dr. Suman Ghosh
Assistant Professor, NIT Rourkela
Rourkela, Odisha, 769008
ghoshsuman2000@gmail.com

ABSTRACT

A numerical investigation has been made to study the behavior of air bubble entrapped through jet impingement. Attempt has been made also been made to understand the combined effect of jet force and buoyancy on the bubble motion. The Finite Volume Method (FVM) with 3D Volume of Fluid (VOF) model has been adopted to formulate the problem. The role played by the turbulence on the movement of air bubble is examined by varying the Reynolds number of the impinging jet as well as by varying the relative positions of the jet and bubble with respect to each other. Number of bubble under jet has also been varied. Phase contours at a specified vertical plane for different time instant have been generated for each of the case studies to visualize the phenomena. The velocity contours and velocity vectors have also been produced at the same plane for better understanding of the motion of the bubble under the jet force and buoyance force.

Keywords: *Multi-Phase flow, Volume of Fluid (VOF), Buoyancy, Finite Volume Method (FVM), Jet Impingement, Air bubble, Interface.*

NOMENCLATURE

ρ Density of the fluid (Kg/m^3)
μ Viscosity of the fluid (Kg/m-s)
C_p Specific heat (J/Kg-K)
K Thermal conductivity (W/m-K)
g Acceleration due to gravity (m/s^2)
k Turbulent kinetic energy (m^2/s^2)
ε Turbulent dissipation rate (m^2/s^3)
σ_k Turbulent Prandtl number for k
σ_ε Turbulent Prandtl number for ε
S_k User-defined source term for k
S_ε User-defined source term for ε
R_e Reynolds number ($\rho vD/\mu$)

1 INTRODUCTION

Problems associated with air bubble entrapped in another liquid media find many practical applications in engineering and science (e.g. air bubble formation in molten metal during metallurgic processes, air bubble entrainment at hydraulic jumps and self-aeration of free jets). The study of motion of air bubble may lead to understand and control the highly complex processes like nucleate boiling and safety of nuclear reactors, where the control of air bubble formed is a serious matter of concern. When air is entrapped in a liquid media in any process or in any application (like jet impingement in a liquid pool), it forms bubble within it, thus the turbulence and jet force plays very important role on the shape, location and velocity of the bubble, which varies with respect to time. Hence the motion, instant shape and location of bubble would be a function of above mentioned parameters. Hence tracking of the motion of the bubble within the liquid pool is very important.

Numerous scientific journals and books are available regarding to this. Investigation has been made by Chanson [1] for the air bubble entrainment at hydraulic jumps with partially developed inflow conditions. A new gas transfer model is presented. Again air-water flow experiments with two free shear layer flows: a vertical supported jet and a horizontal hydraulic jump were conducted by Chanson [2]. The mechanisms of air entrainment by plunging liquid jets are theoretically and experimentally studied by Cummings and Chanson [3-4]. The air bubble diffusion in the near-flow field of both circular and two-dimensional plunging jets is analyzed by them. The process of air entrainment induced by a liquid jet plugging into a mass of relatively quiescent liquid is experimentally and numerically studied by Zhu et al. [5]. Experimentally they have observed that a smooth jet does not entrap air even at relatively high velocities. A rapid temporary increase of the liquid flow rate generates surface disturbances on the jet and consequently large air cavities are formed. Under the action of gravity these cavities collapse and entrapment of bubbles in the liquid occurs. An experimental study of individual air bubble entrainment at a planar plunging jet has been made by Cummings and Chanson [6]. They have reported that at the impact of a plunging liquid jet with a receiving pool, air bubbles may be entrained if the impact velocity exceeds a critical velocity. The effect of nozzle type on air entrainment by plunging water jets has been experimentally investigated by Bagatur et al. [7]. An experimental study of the air entrainment rate of circular nozzles with and without air holes, has been made by Emiroglu and Baylar [8]. Air entrainment and bubble dispersion in the developing flow region of vertical circular plunging jets has been investigated by Chanson et al. [9]. A template-based system for identifying and tracking vapor bubbles, have been developed by Cheng and Burkhardt [10] through an experimental investigation using a high-speed digital camera. A theoretical formulation about energy transformation and dissipation caused by air bubble entrainment in water has been proposed by Hoque and Aoki [11]. A combined experimental and numerical study of the flow characteristics of round vertical liquid jets plunging into a cylindrical liquid bath have been made by Qu et al. [12]. The plunging jet flow patterns, entrained air bubble sizes and the influence of the jet velocity and variations of jet falling lengths on the jet penetration depth have been experimentally determined by them. Numerical study of a bubble plume generated by bubble entrainment from an impinging jet was done by Kendil et al. [13]. A detailed experimental study of a plunging jet on a free liquid surface was made by Qu et al. [14]. Experimental characterization facility was designed and constructed by them for generating vertical round water jet impinging on free surface of a pool.

It could be inferred from the above literature survey that the work done to date investigates only about the mechanism of air entrapment through various activities in liquid media. In order to minimize the air entrapment due to turbulence, jet impingement (in free liquid surface) phenomena are studied at various papers. Unfortunately no much study is found to predict the shape, instant size of the bubble and to track the motion of the bubble entrapped through jet according to the best of the authors' knowledge. Hence there is a need to study the dynamics of air bubble entrapped through jet impingement in the free surface of a liquid pool.

The present study investigates the behavior of air bubble entrapped through jet impingement in a liquid pool under the combined effect of jet force and buoyancy force. In order to understand the mobility of air bubble and to understand the effect of turbulence on bubble shape, bubble size, bubble position and bubble velocity, a number of case studies have been performed by varying Reynolds number, initial location of air bubble, location of jet and the number of air bubble.

2 PROBLEM STATEMENTS

This section deals with the detailed information about the problem with different case studies with suitable schematic diagrams and explanation. In the present paper, a numerical investigation has been made to study the behavior of air bubble entrapped through jet impingement on the free surface of a water pool.

The numerical study is made with a vertical cylindrical tank of 65 mm diameter and 60 mm height, having an impinging jet of 15 mm diameter. The Reynolds number (*Re*) of the jet is varied from 1800 to 4000 in order to understand the effect of turbulence on the movement of air bubble. Air bubble of 3 mm diameter is considered here and the role played by the turbulence is examined by placing the bubble and jet at different locations. Following cases have been studied:

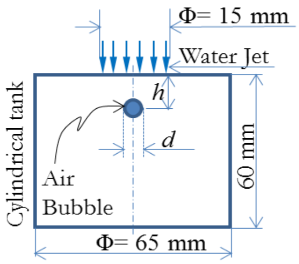

Figure 1. SCHEMATIC REPRESENTATION OF THE BUBBLE AND A JET PLACED AT THE CENTER OF THE TANK (h =10 mm AND d = 3 mm)

2.1 A Bubble and a Jet Placed at the Center of the Tank

A jet is placed at the axis of the tank and a bubble has been placed directly below 10 mm from the free surface of water at the same axis. Figure 1 represents the schematic diagram of the test problem. The effect of variation of jet velocity has been studied by performing the same study for Reynolds number 1800, 2500 and 4000.

2.2 Two Bubbles Placed Either Sides of the Axis of the Tank and a Jet Placed at the Center of the Tank

To understand the air bubble mobility phenomena more clearly this case deals with two air bubbles of the same size (dia: 3 mm) placed either side of the axis of the tank at the same distance from the axis and jet is applied at the center of the tank as shown in Figure 2. This case is repeated for the Reynolds number 2500 and 4000.

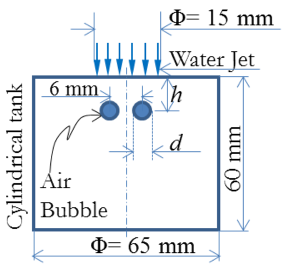

Figure 2. SCHEMATIC REPRESENTATION OF THE TWO BUBBLES PLACED EITHER SIDES OF THE AXIS AND A JET AT THE CENTRE OF TANK (h = 10 mm, d = 3 mm)

2.3 A Bubble Placed with an Eccentricity from the Axis and Jet Placed at the Center of Tank

A bubble is placed with an eccentricity (e) from the axis of the tank and at a vertical distance of 10 mm from the free surface of water. Figure 3 shows the schematic diagram of the problem. Reynolds number for jet is chosen as 4000.

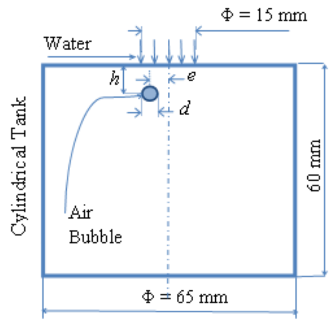

Figure 3. SCHEMATIC REPRESENTATION OF BUBBLE PLACED WITH AN ECCENTRICITY FROM THE AXIS AND JET PLACED AT THE CENTER OF TANK (h = 10 mm, d = 3 mm AND e = 3 mm).

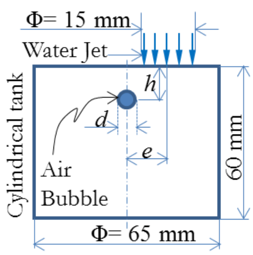

Figure 4: SCHEMATIC REPRESENTATION OF BUBBLE PLACED AT THE CENTRE AND JET PLACED WITH AN ECCENTRICITY FROM THE AXIS (h =10 mm, d =3 mm)

2.4 A Bubble Placed at the Center and a Jet Placed with an Eccentricity from the Axis

Location of jet plays an important role on the mobility of the entrapped bubble. Hence, five different cases have been studied for different locations of the jet with respect to the center of the tank. Figure 4 shows one of these five cases. Reynolds number for jet is chosen as 4000.

2.5 Two Bubbles Placed Vertically on the Axis of the Tank and Jet also Placed at the Center of Tank

This case deals with two air bubbles placed vertically along the axis of the tank separated by a vertical distance of 6 mm. Jet is also placed at the axis of the tank. Figure 5 shows the schematic representation. Same problem is repeated with a vertical distance of 20 mm between the bubbles. Reynolds number for both cases is chosen as 4000.

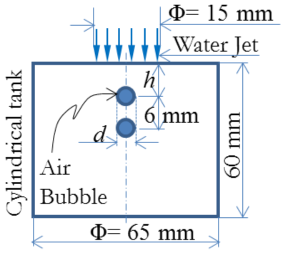

Figure 5: THE SCHEMATIC REPRESENTATION OF THE TWO BUBBLES PLACED VERTICALLY ON THE AXIS OF THE TANK AND JET ALSO PLACED AT THE CENTER OF THE AXIS (h = 10 mm, d =3 mm).

3 NUMERICAL CALCULATIONS

The 3D Finite Volume Method (FVM) with Volume of Fluid (VOF) multiphase model in Fluent 6.3.26 has been used to simulate the problem. The VOF surface tracking technique with pressure-based solver in 3D version has been used to analyze this non-linear and unsteady problem. To simulate the complex interface, the pressure-based implicit splitting of operators (PISO) method has been used. For turbulent modeling k-ε turbulent model is used.

3.1 Grid pattern employed

After an extensive verification by changing the type and size of the grid/mesh keeping the other parameters (size and position of the air bubble) fixed, the 'Hex/Wedge' elements with 'Cooper' type grid have been considered for meshing the geometrical model as shown in Figure 6. Finally for the better shape and size of the spherical air bubble, grid size of 0.0003 m has been chosen through a grid independent test.

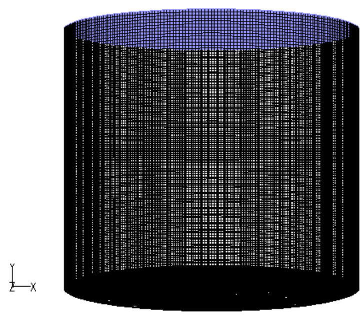

Figure 6. MODELING OF CYLINDRICAL TANK WITH SUITABLE MESH AND BOUNDARY CONDITIONS.

3.2 Governing Equations

The governing equations used in simulation are given below.

3.2.1 The continuity Equation: Continuity equation is derived on the principle of conservation of mass. It is the governing equation in any CFD problem. The continuity equation in the vector form for each of the individual phase is given by;

$$\frac{\partial \rho}{\partial t} + \nabla \cdot (\rho \vec{v}) = 0 \tag{1}$$

3.2.2 The Momentum equation: The VOF model uses a single set of momentum equation with pressure-based solver. The Navier-stroke's or momentum equation for the flow field is given by;

$$\frac{\partial}{\partial t}(\rho \vec{v}) + \nabla \cdot (\rho \vec{v}\vec{v}) = -\nabla p + \nabla \cdot \left[\mu\left(\nabla \vec{v} + \nabla \vec{v}^{\mathrm{T}}\right)\right] + \rho \vec{g} + \vec{F} \tag{2}$$

3.2.3 Turbulent Kinetic Energy (*k*) and Turbulent Dissipation rate (*ε*) model: The turbulence presence in the domain has been modeled using standard ***k*-*ε*** model which are given below;

$$\frac{\partial}{\partial t}(\rho k) + \frac{\partial}{\partial x_i}(\rho k u_i) = \frac{\partial}{\partial x_j}\left[\left(\mu + \frac{\mu_t}{\sigma_k}\right)\frac{\partial k}{\partial x_j}\right] + G_k + G_b - \rho\varepsilon - Y_M + S_k \tag{3}$$

$$\frac{\partial}{\partial t}(\rho \varepsilon) + \frac{\partial}{\partial x_i}(\rho \varepsilon u_i) = \frac{\partial}{\partial x_j}\left[\left(\mu + \frac{\mu_t}{\sigma_\varepsilon}\right)\frac{\partial \varepsilon}{\partial x_j}\right] + C_{1\varepsilon}\frac{\varepsilon}{k}(G_k + C_{3\varepsilon}G_b) - C_{2\varepsilon}\rho\frac{\varepsilon^2}{k} + S_\varepsilon \tag{4}$$

Where G_k represents the generation of turbulence kinetic energy due to the mean velocity gradients, G_b is the generation of turbulence kinetic energy due to buoyancy, Y_M represents the contribution of the fluctuating dilatation in compressible turbulence to the overall dissipation rate. $C_{1\varepsilon}$ and $C_{2\varepsilon}$ are constants. σ_k and σ_ε are the turbulent Prandtl numbers for k and ε, respectively. S_k and S_ε are user-defined source terms. Here μ_t is the turbulent viscosity.

$$\mu_t = \rho C_\mu \frac{k^2}{\varepsilon} \tag{5}$$

where C_μ is a constant. The model constants $C_{1\varepsilon}$, $C_{2\varepsilon}$, $C_{3\varepsilon}$, σ_k and σ_ε have the following default values: $C_{1\varepsilon}$ =1.44, $C_{2\varepsilon}$ =1.92, $C_{3\varepsilon}$ = 0.09, σ_k = 1.0 and σ_ε =1.3.

3.3 Boundary Conditions

The problem has been simulated using appropriate boundary conditions along with all other scalar properties of flow in order to define the actual problems viz.:

3.3.1 *Velocity inlet* Boundary Condition: *Velocity inlet* boundary condition has been used for the jet at the top plane of the cylindrical tank. A uniform velocity profile (u = 0; $v = v_{in}$; w = 0) of the jet has been taken.

3.3.2 *Pressure inlet* boundary condition: *Pressure inlet* boundary condition ($p = p_{atm}$) has been used at the top plane of the cylindrical tank except the jet position.

3.3.3 *Wall* boundary condition: *Wall* boundary condition has been used for the remaining planes (i.e. circumference and bottom plane) of the cylindrical tank. In the *Wall* boundary condition, no-slip and no-penetration conditions have been used.

3.4 Residuals and convergence

In order to increase the accuracy of the solution all the scaled residuals value (for continuity, x-velocity, y-velocity, z-

velocity, k and ε) have been set below a sufficiently small value of 10^{-6}.

4 RESULTS AND DISCUSSIONS

This section deals with the results obtained and the corresponding discussion for the selected case studies. For turbulence modeling the turbulence parameters were set as, turbulent kinetic energy (k) = 0.0225 m^2/s^2, turbulent dissipation rate (ε) = 0.00792 m^2/s^3. The fluid properties were set as, surface tension at air-water interface = 0.0736 N/m, density of water = 998.2 kg/m^3, viscosity = 0.001003 Pa-s. For each of the case studies, the air bubble diameter is considered as 3 mm and jet diameter is taken as 15 mm. The Reynolds number (Re) of the jet has been varied from 1800 to 4000.

After numerical simulation, phase contours, velocity contours and velocity vector plot have been produced at the vertical mid plane of the cylindrical tank at each time step with a step size of 0.0001 second. These contours and plots show the shape, position and velocity of the air bubble at different time instants and variations of shape, position and velocity with time. The results of all the case studies are explained with the corresponding phase contour, velocity contours and velocity vector plot at different time instants. These results are given below case wise.

4.1 A Bubble and A Jet Placed at the Centre of the Tank

Here, the jet is placed along the axis of the tank and bubble is placed just below 10 mm from the free surface of water at the same axis. This case study has been repeated for three different Reynolds number (Re = 1800, Re = 2500 and Re = 4000).

4.1.1 *Re* =1800: As the air bubble do not feel the downward jet force suddenly at the starting condition (some time is required to reach the jet effect at the bubble position from the free surface) it starts moving in the upward direction due to buoyancy effect. It reaches up to certain height within the tank and stabilizes there when it comes in equilibrium under the buoyancy force and jet force. The air bubble frequently changes its shape there in order to resist the imbalance of buoyancy and jet forces on its surface. Figure 7 shows the phase contours at the vertical mid plane of the tank at different time instant.

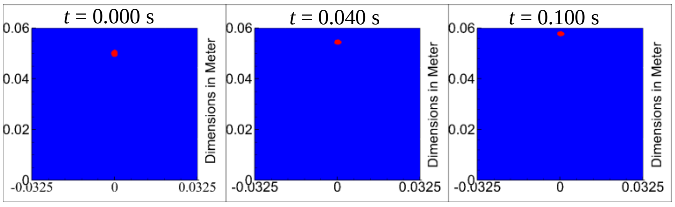

FIGURE 7. PHASE CONTOURS AT THE VERTICAL MIDDLE PLANE (A BUBBLE AND A JET PLACED AT THE CENTER OF THE TANK WITH *Re* =1800).

4.1.2 *Re* = 2500: A turbulent jet with Reynolds number of 2500 is used keeping the positions of jet and bubble unaltered. At the beginning of impingement, jet force is not experienced by the bubble (as some time is required to reach the jet effect at the bubble position from the free surface of water), hence it starts to move in the upward direction due to the buoyancy force alone. But after gaining some height, it experiences jet force as well. Due to the imbalance between the dominating jet force and buoyancy force, air bubble now slowly starts moving in the downward direction. Figure 8 and 9 shows the phase contour and velocity vector plot respectively at the vertical mid plane of the tank.

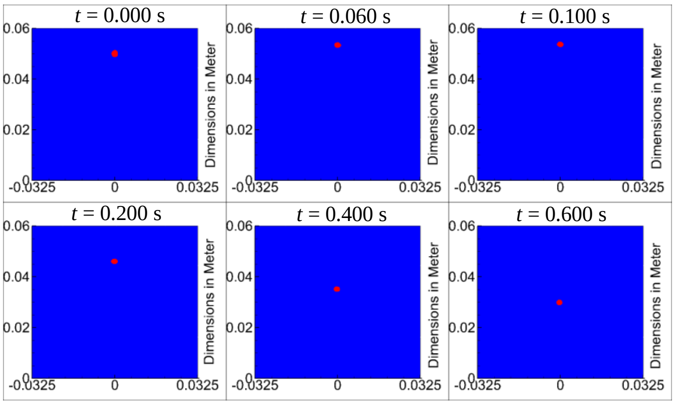

Figure 8. PHASE CONTOURS AT THE VERTICAL MIDDLE PLANE (A BUBBLE AND JET PLACED AT THE CENTER OF THE TANK WITH *Re* =2500).

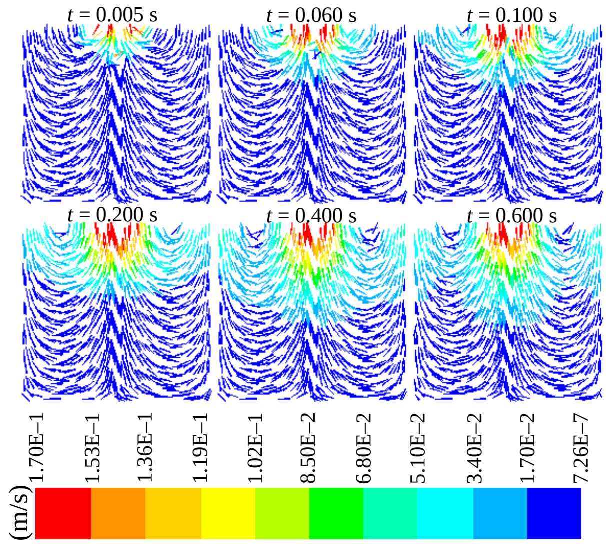

Figure 9. VELOCITY (m/s) VECTORS AT THE VERTICAL MIDDLE PLANE (A BUBBLE AND A JET PLACED AT THE CENTER OF THE TANK WITH *Re* =2500).

4.1.3 *Re* =4000: To understand the effect of turbulence more effectively, a greater value of Reynolds number has been taken as 4000. Initially the bubble try to move in upward direction very slowly but as it senses the jet force (with in a short while) it start to move downward direction more quickly as compared to previous case because of higher jet force. The phase and velocity contours at the vertical mid plane are shown below in Figure 10 and 11 respectively.

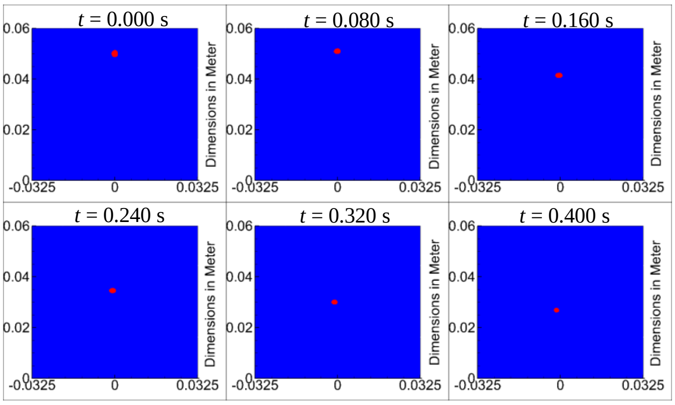

Figure 10. PHASE CONTOURS ON VERTICAL MIDDLE PLANE (A BUBBLE AND A JET PLACED AT THE CENTER OF THE TANK WITH *Re* = 4000).

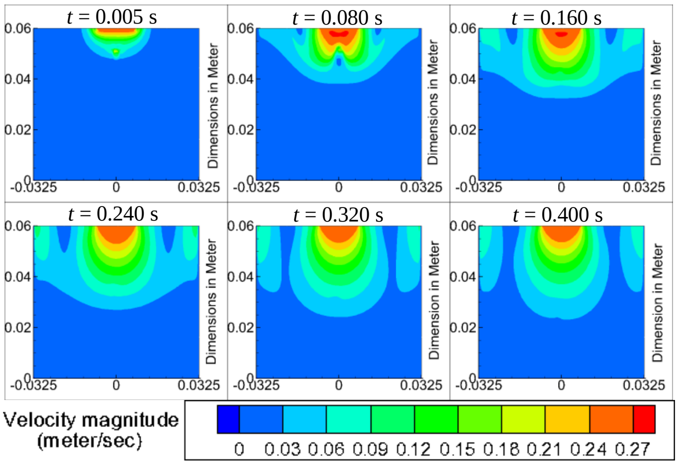

Figure 11. VELOCITY(m/s) CONTOURS ON VERTICAL MIDDLE PLANE (A BUBBLE AND A JET PLACED AT THE CENTER OF THE TANK WITH *Re* = 4000).

4.2 Two Bubbles Placed Either Sides of the Axis of the Tank and a Jet Placed along the Axis of the Tank

Two air bubbles are horizontally placed in either side of the axis of the tank maintaining a distance 6 mm between the centers of the bubbles. The jet is again placed along the axis of the tank. Both the bubbles are kept 10 mm below the top of the tank and have been considered under the jet impingement. This study has been repeated for two Reynolds numbers 2500 and 4000. Figure 12 and 13 shows the results of this study for the Reynolds number of 2500 in terms of phase contour and velocity contour at different time instants.

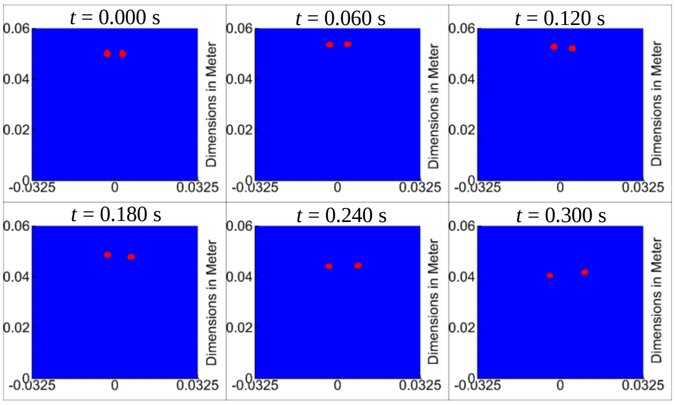

Figure 12. PHASE CONTOURS ON VERTICAL MID PLANE (TWO BUBBLES PLACED EITHER SIDE OF THE AXIS AND A JET PLACED ALONG AT THE CENTER WITH *Re* = 2500.)

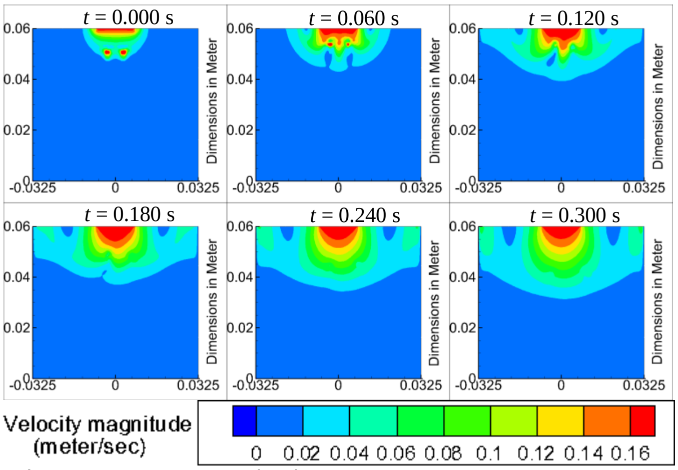

Figure 13: VELOCITY (m/s) CONTOURS ON VERTICAL MID PLANE (TWO BUBBLES PLACED EITHER SIDE OF THE AXIS AND A JET PLACED AT THE CENTER OF THE TANK WITH *Re* = 2500.)

At first both the bubbles tends to move upward direction due to the buoyancy effect (as initially jet force is not sensed by the bubbles), but slowly there velocity retards and they move downward direction due to the dominating jet force. The effect of turbulence is varying place to place. Both the bubbles follow different curved paths to move further. Same phenomena repeated at *Re* = 4000, but here bubbles move downward direction in a faster way.

4.3 A Bubble Placed with an Eccentricity from the Axis and Jet Placed at the Center of the Tank

A single jet (with *Re* =4000) and a single bubble are used here. The jet is placed again along the center of the axis of the tank but the bubble is placed with an eccentricity of 3 mm from the axis (horizontal distance of 3 mm from the axis) and 10 mm vertical distance from the free surface of water. The results of this case study are shown in Figure 14 in terms of the phase contours at the vertical mid plane at different time instants. The bubble again initially moves in upward direction up to certain height. But it feels the jet force very soon as in the previous cases and then it moves towards the bottom following a curve path unlike the case 4.3.1 where the bubble moves in a straight path. Figure 15 shows the velocity vector plot on the vertical mid plan at different time instant for this case study.

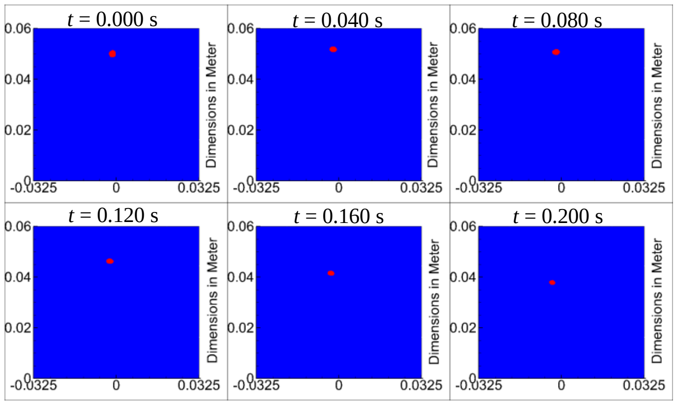

Figure 14. PHASE CONTOURS ON VERTICAL MIDDLE PLANE (BUBBLE PLACED WITH AN ECCENTRICITY OF 3 mm FROM THE AXIS AND JET PLACED ALONG THE AXIS OF THE TANK. *Re* = 4000).

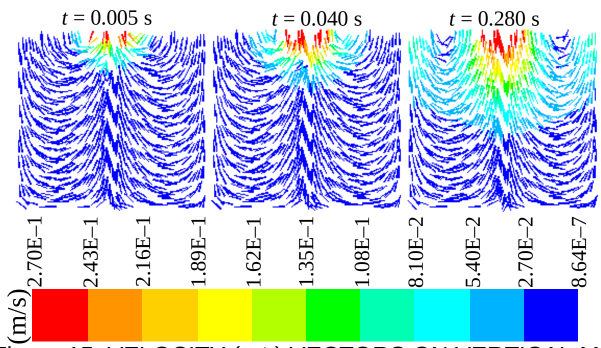

Figure 15. VELOCITY (m/s) VECTORS ON VERTICAL MID PLANE AT DIFFERENT TIME INSTANT (BUBBLE PLACED WITH AN ECCENTRICITY OF 3 mm FROM THE AXIS AND JET PLACED AT THE CENTER, *Re* = 4000).

4.4 A Bubble Placed at the Center of the Axis and Jet Placed with an Eccentricity from the Axis of the Tank

In this case an air bubble has been placed at the center of the tank and 10 mm vertical distance from the free surface (as shown in Figure 4). Jet is placed with an eccentricity from the axis (horizontal distance from the axis) of the tank. Figure 16 shows the results of this study in terms of phase contours at the vertical mid plane at different time instant for the eccentricity value e =10 mm. As the line of action of the jet is away from the bubble center, the jet force cannot directly influence the bubble hence buoyancy force dominating the bubble motion. But, here bubble is close to the line of action of the jet so it feels buoyancy force and jet force as well. Hence it follows an inclined path to move in upward direction, and then moves out to the atmosphere. This study has been repeated by varying the horizontal distance of the jet (eccentricity) from the axis. It has been observed that when the line of action of the jet is very away from the bubble-center, bubble moves out in the atmosphere in a straight vertical path before experiencing the jet force. But as the line of action of the jet comes closer to the bubble center, the bubble no more moves in straight vertical path but in an inclined path to escape in atmosphere. The inclination of path increases as the eccentricity reduces. The velocity contours at the vertical mid plane at different time instant for this study (e = 10 mm) are shown in Figure 17.

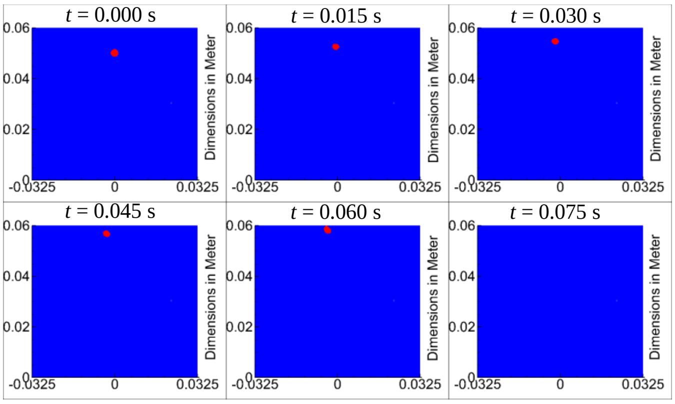

Figure 16. PHASE CONTOURS AT THE VERTICAL MID PLANE (A BUBBLE AT THE CENTER OF THE TANK AND JET WITH AN ECCENTRICITY OF 10 mm, Re = 4000).

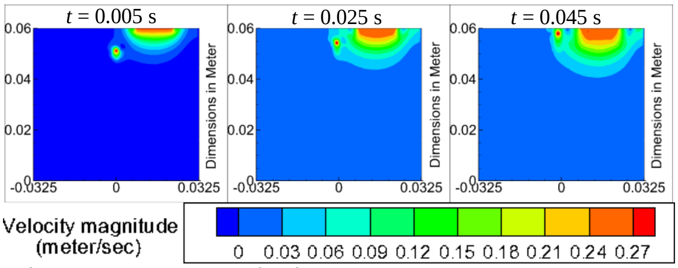

Figure 17: VELOCITY (m/s) CONTOURS AT THE VERTICAL MIDDLE PLANE (A BUBBLE AT THE CENTER OF THE TANK AND JET WITH AN ECCENTRICITY OF 10 mm, Re =4000).

4.5 Two Bubbles Placed Vertically on the Center of the Axis of the Tank and Jet also Placed at the Center of the Axis of the tank

In this study, two bubbles are placed vertically along the axis of the tank and a turbulent jet of Reynolds number 4000 is also placed along the axis of the tank (as shown in Figure 5). This case study is repeated twice by varying the vertical distance between the centers of the bubbles (6 mm and 20 mm). For both case, the jet diameter is considered as 15 mm and bubble diameter is considered as 3 mm. Again for both case, upper bubble is placed at 10 mm below the free surface of the water.

4.5.1 Bubbles separated by 6 mm: Results for this case are given in Figure 18 in terms of the phase contours at the vertical mid plane of the tank for different time instant. At the beginning, both the bubble initially experiences buoyancy force and do not feels the jet impact suddenly. As a result, air bubbles initially tend to move upward direction. The upper bubble stabilized at a certain height from its initial position and lower bubble get merge into it and form a new large bubble. Then this large bubble slowly moves in the vertical downward direction.

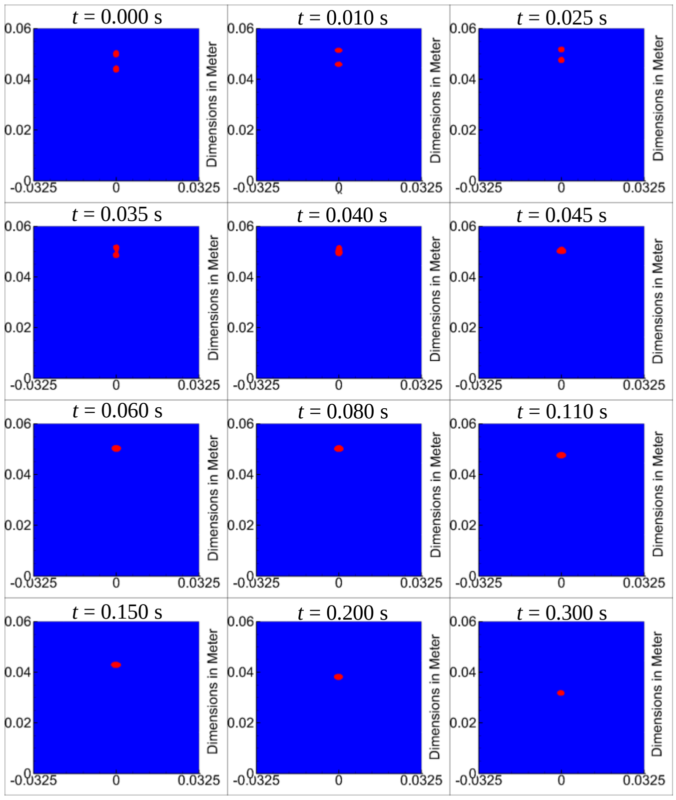

Figure 18: PHASE CONTOURS ON VERTICAL MID PLANE FOR VERTICALLY 6 mm SEPARATED BUBBLES (Re =4000).

4.5.2 Bubbles separated by 20 mm: Results for this case are shown in Figure 19 and 20. Figure 19 shows the phase contours and Figure 20 shows the velocity contours at the vertical mid plane of the tank for different time instants.

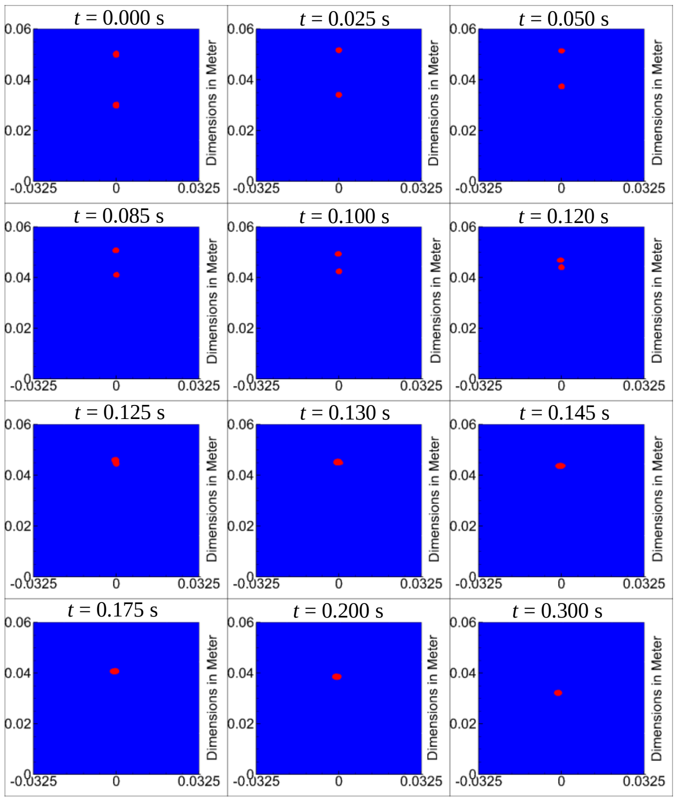

Figure 19: PHASE CONTOURS ON VERTICAL MID PLANE FOR VERTICALLY 20 mm SEPARATED BUBBLES (Re=4000)

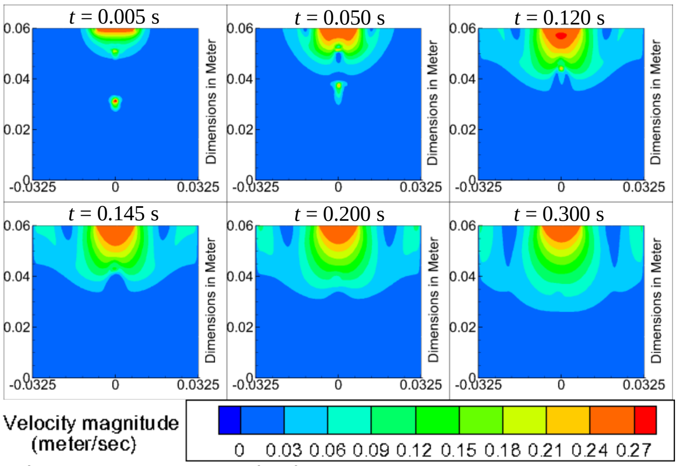

Figure 20. VELOCITY (m/s) CONTOURS ON VERTICAL MID PLANE FOR VERTICALLY 20 mm SEPARATED BUBBLES (Re = 4000).

Initially both the bubbles tends to move upward direction but due the jet force, upper bubble stabilizes after gaining some height for a moment and then starts moving in downward direction. But lower one keeps moving in upward direction due to buoyancy force alone as it is in very deep position in the tank and hence do not feels the jet force. It can also be observed from velocity contours shown in Figure 20. After some time-steps, both the bubbles (which are moving in the opposite direction relative to each other) merges and forms a bigger bubble which moves in downward direction following a curved path due to turbulence.

5 CONCLUSIONS

An attempt has been made to predict the mobility and behavior of air bubble within a liquid pool entrapped through jet impingement. The test problem has been numerically simulated using the Finite Volume Method (FVM) with 3D Volume of Fluid (VOF) model. Both laminar and turbulent jets have been considered. In order to get the role of turbulence in the bubble motion and shape the Reynolds number of the impinging jet has been varied in a wide range. The number of bubble and the locations of jet and bubble have also been varied for better understanding. For each of the case studies, phase contours have been extracted at the vertical mid plane of the tank for each time step of the simulation in order to get the variations of shape, position and velocity of the air bubble with time. The velocity contours and velocity vector plots have also been produced at the same plane for better understanding of the motion of the bubble. By observing these contours following conclusions can be made.

- The shape and location of the air bubble under the jet are strongly depended on the Reynolds number of the jet.
- The air bubble placed very deep inside the tank experiences the jet force much later as compared to the bubble placed close to the free surface.
- When the bubble is placed away from the line of the action of jet it feels the jet force from side (not directly) hence moves in an inclined curve path. As the position of jet is kept close to the bubble its inclination increases.
- It can also be concluded that the turbulence plays a vital role on the motion of air bubble as it forces the bubble to follow a curved path instead of straight vertical path.

Moreover it can be said that the present study may lead to understand various process in which a bubble entraps in liquid medium under jet impingement, like hydraulic jump, nucleate boiling, bubble formation in molten metal during metallurgic processes etc. The cases examined here deals with the vertical jet impingement. The effect of inclined or horizontal jet impingement can also be studied in order to predict the behavior of air bubble.

REFERENCES

[1] Chanson, H., 1995. Air-water gas transfer at hydraulic jump with partially developed inflow. *Water Research*, 29(10), October, pp. 2247-2254.

[2] Chanson, H., 1995. Air entrainment in two-dimensional turbulent shear flows with partially developed inflow conditions. *International Journal of Multiphase Flow*, 21(6), November, pp. 1107-1121.

[3] Cummings, P.D., and Chanson, H., 1997a. Air entrainment in the developing flow region of plunging jets–Part 1: Theoretical Development. *Journal of Fluids Engineering*. 119(3), pp. 597-602.

[4] Cummings, P.D., and Chanson, H., 1997b. Air entrainment in the developing flow region of plunging jets–Part 2: Experimental. *Journal of Fluids Engineering*. 119(3), pp. 603-608.

[5] Zhu, Y., Oguz, H. N., and Prosperetti, A., 1998. Mechanism of air entrainment by an impinging liquid jet. *13th Australasian Fluid Mechanics Conference*, Monash University, Melbourne, Australia, 13-18 December, pp. 337-340.

[6] Cummings, P.D. and Chanson, H., 1999. An experimental study of individual air bubble entrainment at a planar plunging jet. *Chemical Engineering Research and Design*, 77(2), March, pp. 159-164..

[7] Bagatur, T., Bayler, A., and Sekerdag, N., 2002. The Effect of Nozzle Type on Air Entrainment by Plunging Water Jets. Water Quality Research Journal of Canada, 37(3), July, pp. 599-612.

[8] Emiroglu, M. E., and Bayler, A., 2003. Role of nozzles with air holes in air entrainment by a water jet. *Water Quality Research Journal of Canada*, 38(4), October, pp. 785-795.

[9] Chanson, H., Aoki, S., and Hoque, A., 2004. Physical modelling and similitude of air bubble entrainment at vertical circular plunging jets. *Chemical Engineering Science*, 59(4), pp. 747-758.

[10] Cheng, D.C., and Burkhardt, H., 2006. Tracki Template-based bubble identification and tracking in image sequences. *International Journal of Thermal Sciences*, 45(3), March, pp. 321-330.

[11] Hoque, A., and Aoki, S., 2008. Air entrainment and associated energy dissipation in steady and unsteady plunging jets at free surface. *Applied Ocean Research*, 30(1), February, pp. 37-45.

[12] Qu, X. L., Khezzar, L., Danciu, D., Labois, M., and Lakehal, D., 2011. Characterization of plunging liquid jets: A combined experimental and numerical investigation. *International Journal of Multiphase Flow*, 37(7), September, pp. 722-731.

[13] Kendil, F.Z., Krepper E., Salah A., Lucas D., and Mataoui A., 2011. Numerical study of a bubble plume generated by bubble entrainment from an impinging jet. *Nuclear Engineering and Design*, 241(10), October, pp. 4111-4121.

[14] Qu, X., Goharzadeh, A., Khezzar, L., and Molki, A., 2013, Experimental characterization of air-entrainment in a plunging jet. *Experimental Thermal and Fluid Science*, 44, January, pp. 51-61.